Observation of Two-Source Interference in the Photoproduction Reaction AuAu → AuAu ρ0

(STAR Collaboration) Abelev, B. I.; ...; Planinić, Mirko; ...; Poljak, Nikola; ...; Zuo, J. X.

Journal article, Published version
Rad u časopisu, Objavljena verzija rada (izdavačev PDF)

Permanent link / Trajna poveznica: https://urn.nsk.hr/urn:nbn:hr:217:412883

Download date / Datum preuzimanja: **2024-04-25**

Repository / Repozitorij:

Repository of the Faculty of Science - University of Zagreb

P H Y S I C A L   R E V I E W   L E T T E R S

Observation of Two-Source Interference in the Photoproduction Reaction $AuAu \rightarrow AuAu\rho^0$

B. I. Abelev,[9] M. M. Aggarwal,[31] Z. Ahammed,[47] B. D. Anderson,[19] D. Arkhipkin,[13] G. S. Averichev,[12] Y. Bai,[28] J. Balewski,[23] O. Barannikova,[9] L. S. Barnby,[2] J. Baudot,[17] S. Baumgart,[52] D. R. Beavis,[3] R. Bellwied,[50] F. Benedosso,[28] M. J. Betancourt,[23] R. R. Betts,[9] S. Bhardwaj,[36] A. Bhasin,[18] A. K. Bhati,[31] H. Bichsel,[49] J. Bielcik,[11] J. Bielcikova,[11] B. Biritz,[6] L. C. Bland,[3] M. Bombara,[2] B. E. Bonner,[37] M. Botje,[28] J. Bouchet,[19] E. Braidot,[28] A. V. Brandin,[26] E. Bruna,[52] S. Bueltmann,[30] T. P. Burton,[2] M. Bystersky,[11] X. Z. Cai,[40] H. Caines,[52] M. Calderón de la Barca Sánchez,[5] J. Callner,[9] O. Catu,[52] D. Cebra,[5] R. Cendejas,[6] M. C. Cervantes,[42] Z. Chajecki,[29] P. Chaloupka,[11] S. Chattopadhyay,[47] H. F. Chen,[39] J. H. Chen,[40] J. Y. Chen,[51] J. Cheng,[44] M. Cherney,[10] A. Chikanian,[52] K. E. Choi,[35] W. Christie,[3] S. U. Chung,[3] R. F. Clarke,[42] M. J. M. Codrington,[42] J. P. Coffin,[17] R. Corliss,[23] T. M. Cormier,[50] M. R. Cosentino,[38] J. G. Cramer,[49] H. J. Crawford,[4] D. Das,[5] S. Dash,[14] M. Daugherity,[43] C. De Silva,[50] T. G. Dedovich,[12] M. DePhillips,[3] A. A. Derevschikov,[33] R. Derradi de Souza,[7] L. Didenko,[3] P. Djawotho,[42] S. M. Dogra,[18] X. Dong,[22] J. L. Drachenberg,[42] J. E. Draper,[5] F. Du,[52] J. C. Dunlop,[3] M. R. Dutta Mazumdar,[47] W. R. Edwards,[22] L. G. Efimov,[12] E. Elhalhuli,[2] M. Elnimr,[50] V. Emelianov,[26] J. Engelage,[4] G. Eppley,[37] B. Erazmus,[41] M. Estienne,[17] L. Eun,[32] P. Fachini,[3] R. Fatemi,[20] J. Fedorisin,[12] A. Feng,[51] P. Filip,[13] E. Finch,[52] V. Fine,[3] Y. Fisyak,[3] C. A. Gagliardi,[42] L. Gaillard,[2] D. R. Gangadharan,[6] M. S. Ganti,[47] E. Garcia-Solis,[9] V. Ghazikhanian,[6] P. Ghosh,[47] Y. N. Gorbunov,[10] A. Gordon,[3] O. Grebenyuk,[22] D. Grosnick,[46] B. Grube,[35] S. M. Guertin,[6] K. S. F. F. Guimaraes,[38] A. Gupta,[18] N. Gupta,[18] W. Guryn,[3] B. Haag,[5] T. J. Hallman,[3] A. Hamed,[42] J. W. Harris,[52] W. He,[16] M. Heinz,[52] S. Heppelmann,[32] B. Hippolyte,[17] A. Hirsch,[34] E. Hjort,[22] A. M. Hoffman,[23] G. W. Hoffmann,[43] D. J. Hofman,[9] R. S. Hollis,[9] H. Z. Huang,[6] T. J. Humanic,[29] G. Igo,[6] A. Iordanova,[9] P. Jacobs,[22] W. W. Jacobs,[16] P. Jakl,[11] F. Jin,[40] C. L. Jones,[23] P. G. Jones,[2] J. Joseph,[19] E. G. Judd,[4] S. Kabana,[41] K. Kajimoto,[43] K. Kang,[44] J. Kapitan,[11] M. Kaplan,[8] D. Keane,[19] A. Kechechyan,[12] D. Kettler,[49] V. Yu. Khodyrev,[33] D. P. Kikola,[22] J. Kiryluk,[22] A. Kisiel,[29] S. R. Klein,[22] A. G. Knospe,[52] A. Kocoloski,[23] D. D. Koetke,[46] M. Kopytine,[19] L. Kotchenda,[26] V. Kouchpil,[11] P. Kravtsov,[26] V. I. Kravtsov,[33] K. Krueger,[1] M. Krus,[11] C. Kuhn,[17] L. Kumar,[31] P. Kurnadi,[6] M. A. C. Lamont,[3] J. M. Landgraf,[3] S. LaPointe,[50] J. Lauret,[3] A. Lebedev,[3] R. Lednicky,[13] C-H. Lee,[35] W. Leight,[23] M. J. LeVine,[3] C. Li,[38] N. Li,[51] Y. Li,[44] G. Lin,[52] S. J. Lindenbaum,[27] M. A. Lisa,[29] F. Liu,[51] H. Liu,[5] J. Liu,[37] L. Liu,[51] T. Ljubicic,[3] W. J. Llope,[37] R. S. Longacre,[3] W. A. Love,[3] Y. Lu,[39] T. Ludlam,[3] D. Lynn,[3] G. L. Ma,[40] Y. G. Ma,[40] D. P. Mahapatra,[14] R. Majka,[52] O. I. Mall,[5] L. K. Mangotra,[18] R. Manweiler,[46] S. Margetis,[19] C. Markert,[43] H. S. Matis,[22] Yu. A. Matulenko,[33] T. S. McShane,[10] A. Meschanin,[33] R. Milner,[23] N. G. Minaev,[33] S. Mioduszewski,[42] A. Mischke,[28] J. Mitchell,[37] B. Mohanty,[47] D. A. Morozov,[33] M. G. Munhoz,[38] B. K. Nandi,[15] C. Nattrass,[52] T. K. Nayak,[47] J. M. Nelson,[2] C. Nepali,[19] P. K. Netrakanti,[34] M. J. Ng,[4] L. V. Nogach,[33] S. B. Nurushev,[33] G. Odyniec,[22] A. Ogawa,[3] H. Okada,[3] V. Okorokov,[26] D. Olson,[22] M. Pachr,[11] B. S. Page,[16] S. K. Pal,[47] Y. Pandit,[19] Y. Panebratsev,[12] T. Pawlak,[48] T. Peitzmann,[28] V. Perevoztchikov,[3] C. Perkins,[4] W. Peryt,[48] S. C. Phatak,[14] M. Planinic,[53] J. Pluta,[48] N. Poljak,[53] A. M. Poskanzer,[22] B. V. K. S. Potukuchi,[18] D. Prindle,[49] C. Pruneau,[50] N. K. Pruthi,[31] J. Putschke,[52] R. Raniwala,[36] S. Raniwala,[36] R. L. Ray,[43] R. Redwine,[23] R. Reed,[5] A. Ridiger,[26] H. G. Ritter,[22] J. B. Roberts,[37] O. V. Rogachevskiy,[12] J. L. Romero,[5] A. Rose,[22] C. Roy,[41] L. Ruan,[3] M. J. Russcher,[28] V. Rykov,[19] R. Sahoo,[41] I. Sakrejda,[22] T. Sakuma,[23] S. Salur,[22] J. Sandweiss,[52] M. Sarsour,[42] J. Schambach,[43] R. P. Scharenberg,[34] N. Schmitz,[24] J. Seger,[10] I. Selyuzhenkov,[16] P. Seyboth,[24] A. Shabetai,[17] E. Shahaliev,[12] M. Shao,[39] M. Sharma,[50] S. S. Shi,[51] X-H. Shi,[40] E. P. Sichtermann,[22] F. Simon,[24] R. N. Singaraju,[47] M. J. Skoby,[34] N. Smirnov,[52] R. Snellings,[28] P. Sorensen,[3] J. Sowinski,[16] H. M. Spinka,[1] B. Srivastava,[34] A. Stadnik,[12] T. D. S. Stanislaus,[46] D. Staszak,[6] M. Strikhanov,[26] B. Stringfellow,[34] A. A. P. Suaide,[38] M. C. Suarez,[9] N. L. Subba,[19] M. Sumbera,[11] X. M. Sun,[22] Y. Sun,[39] Z. Sun,[21] B. Surrow,[23] T. J. M. Symons,[22] A. Szanto de Toledo,[38] J. Takahashi,[7] A. H. Tang,[3] Z. Tang,[39] T. Tarnowsky,[34] D. Thein,[43] J. H. Thomas,[22] J. Tian,[40] A. R. Timmins,[2] S. Timoshenko,[26] D. Tlusty,[11] M. Tokarev,[12] T. A. Trainor,[49] V. N. Tram,[22] A. L. Trattner,[4] S. Trentalange,[6] R. E. Tribble,[42] O. D. Tsai,[6] J. Ulery,[34] T. Ullrich,[3] D. G. Underwood,[1] G. Van Buren,[3] M. van Leeuwen,[28] A. M. Vander Molen,[25] J. A. Vanfossen, Jr.,[19] R. Varma,[15] G. M. S. Vasconcelos,[7] I. M. Vasilevski,[13] A. N. Vasiliev,[33] F. Videbaek,[3] S. E. Vigdor,[16] Y. P. Viyogi,[14] S. Vokal,[12] S. A. Voloshin,[50] M. Wada,[43] W. T. Waggoner,[10] M. Walker,[23] F. Wang,[34] G. Wang,[6] J. S. Wang,[21] Q. Wang,[34] X. Wang,[44] X. L. Wang,[39] Y. Wang,[44] J. C. Webb,[46] G. D. Westfall,[25] C. Whitten, Jr.,[6] H. Wieman,[22] S. W. Wissink,[16] R. Witt,[45] Y. Wu,[51] W. Xie,[34] N. Xu,[22] Q. H. Xu,[22] Y. Xu,[39] Z. Xu,[3] P. Yepes,[37] I-K. Yoo,[35] Q. Yue,[44] M. Zawisza,[48] H. Zbroszczyk,[48] W. Zhan,[21] H. Zhang,[3] S. Zhang,[40] W. M. Zhang,[19] Y. Zhang,[39] Z. P. Zhang,[39] Y. Zhao,[39] C. Zhong,[40] J. Zhou,[37] R. Zoulkarneev,[13] Y. Zoulkarneeva,[13] and J. X. Zuo[40]

(STAR Collaboration)

[1]*Argonne National Laboratory, Argonne, Illinois 60439, USA*
[2]*University of Birmingham, Birmingham, United Kingdom*
[3]*Brookhaven National Laboratory, Upton, New York 11973, USA*
[4]*University of California, Berkeley, California 94720, USA*
[5]*University of California, Davis, California 95616, USA*
[6]*University of California, Los Angeles, California 90095, USA*
[7]*Universidade Estadual de Campinas, Sao Paulo, Brazil*
[8]*Carnegie Mellon University, Pittsburgh, Pennsylvania 15213, USA*
[9]*University of Illinois at Chicago, Chicago, Illinois 60607, USA*
[10]*Creighton University, Omaha, Nebraska 68178, USA*
[11]*Nuclear Physics Institute AS CR, 250 68 Řež/Prague, Czech Republic*
[12]*Laboratory for High Energy (JINR), Dubna, Russia*
[13]*Particle Physics Laboratory (JINR), Dubna, Russia*
[14]*Institute of Physics, Bhubaneswar 751005, India*
[15]*Indian Institute of Technology, Mumbai, India*
[16]*Indiana University, Bloomington, Indiana 47408, USA*
[17]*Institut de Recherches Subatomiques, Strasbourg, France*
[18]*University of Jammu, Jammu 180001, India*
[19]*Kent State University, Kent, Ohio 44242, USA*
[20]*University of Kentucky, Lexington, Kentucky, 40506-0055, USA*
[21]*Institute of Modern Physics, Lanzhou, China*
[22]*Lawrence Berkeley National Laboratory, Berkeley, California 94720, USA*
[23]*Massachusetts Institute of Technology, Cambridge, Massachusetts 02139-4307, USA*
[24]*Max-Planck-Institut für Physik, Munich, Germany*
[25]*Michigan State University, East Lansing, Michigan 48824, USA*
[26]*Moscow Engineering Physics Institute, Moscow, Russia*
[27]*City College of New York, New York, New York 10031, USA*
[28]*NIKHEF and Utrecht University, Amsterdam, The Netherlands*
[29]*Ohio State University, Columbus, Ohio 43210, USA*
[30]*Old Dominion University, Norfolk, Virginia, 23529, USA*
[31]*Panjab University, Chandigarh 160014, India*
[32]*Pennsylvania State University, University Park, Pennsylvania 16802, USA*
[33]*Institute of High Energy Physics, Protvino, Russia*
[34]*Purdue University, West Lafayette, Indiana 47907, USA*
[35]*Pusan National University, Pusan, Republic of Korea*
[36]*University of Rajasthan, Jaipur 302004, India*
[37]*Rice University, Houston, Texas 77251, USA*
[38]*Universidade de Sao Paulo, Sao Paulo, Brazil*
[39]*University of Science and Technology of China, Hefei 230026, China*
[40]*Shanghai Institute of Applied Physics, Shanghai 201800, China*
[41]*SUBATECH, Nantes, France*
[42]*Texas A&M University, College Station, Texas 77843, USA*
[43]*University of Texas, Austin, Texas 78712, USA*
[44]*Tsinghua University, Beijing 100084, China*
[45]*United States Naval Academy, Annapolis, Maryland 21402, USA*
[46]*Valparaiso University, Valparaiso, Indiana 46383, USA*
[47]*Variable Energy Cyclotron Center, Kolkata 700064, India*
[48]*Warsaw University of Technology, Warsaw, Poland*
[49]*University of Washington, Seattle, Washington 98195, USA*
[50]*Wayne State University, Detroit, Michigan 48201, USA*
[51]*Institute of Particle Physics, CCNU (HZNU), Wuhan 430079, China*
[52]*Yale University, New Haven, Connecticut 06520, USA*
[53]*University of Zagreb, Zagreb, HR-10002, Croatia*

In ultraperipheral relativistic heavy-ion collisions, a photon from the electromagnetic field of one nucleus can fluctuate to a quark-antiquark pair and scatter from the other nucleus, emerging as a ρ^0. The ρ^0 production occurs in two well-separated (median impact parameters of 20 and 40 F for the cases considered here) nuclei, so the system forms a two-source interferometer. At low transverse momenta, the two amplitudes interfere destructively, suppressing ρ^0 production. Since the ρ^0 decays before the production amplitudes from the two sources can overlap, the two-pion system can only be described

with an entangled nonlocal wave function, and is thus an example of the Einstein-Podolsky-Rosen paradox. We observe this suppression in 200 GeV per nucleon-pair gold-gold collisions. The interference is 87% ± 5%(stat.) ± 8%(syst.) of the expected level. This translates into a limit on decoherence due to wave function collapse or other factors of 23% at the 90% confidence level.

Relativistic heavy ions carry strong electromagnetic fields which can be treated as sources of quasireal virtual photons. When two ions collide, a large variety of two-photon and photonuclear interactions can occur [1]. In coherent vector meson photoproduction, a photon from the field of one nucleus fluctuates into a virtual quark-antiquark pair which scatters elastically from the other nucleus, emerging as a real vector meson. ρ^0 photoproduction has a large cross section, 8%–10% of the hadronic cross section for gold-gold collisions at a center-of-mass energy of 200 GeV per nucleon pair [2–4]. Photoproduction can occur at large impact parameters, b. For ρ^0 photoproduction the median b is about 46 fm [5].

The $(q\bar{q})N$ scattering that produces ρ^0 occurs via the short-ranged strong force; the ρ^0 is produced within one of the two ions. The ρ^0 source consists of two well-separated nuclei. There are two possibilities: either nucleus 1 emits a photon which scatters off nucleus 2 or vice versa. These two possibilities are indistinguishable, and are related by a parity transformation. Vector mesons have negative parity, so the two amplitudes combine with opposite signs. The nuclear separation can be accounted for with a transverse momentum (p_T) dependent phase factor. The cross section is [6]

$$\sigma(p_T, b, y) = |A(p_T, b, y) - A(p_T, b, -y) \exp(i\vec{p}_T \cdot \vec{b})|^2, \tag{1}$$

where $A(p_T, b, y)$ and $A(p_T, b, -y)$ are the amplitudes at rapidity y for ρ^0 production from the two photon directions. We take $\hbar = c = 1$ here. At midrapidity the amplitudes for the two directions are equal, and

$$\sigma(p_T, b, 0) = 2|A(p_T, b, 0)|^2[1 - \cos(\vec{p}_T \cdot \vec{b})]. \tag{2}$$

The system acts as a 2-slit interferometer, with slit separation $b = |\vec{b}|$. The cross sections at different $\vec{b}$ are added, and the p_T spectrum is obtained by integrating Eq. (1) over $\vec{b}$. ρ^0 production is suppressed for $p_T \lesssim 1/\langle b \rangle$, where $\langle b \rangle$ is the mean impact parameter.

The ρ^0 rapidity y and mass m_V and the photon energy k_i are related by $k_{1,2} = (m_V/2) \exp(\pm y)$ where the subscript refers to the two directions. Away from $y = 0$, $k_1 \neq k_2$, so $A(p_T, b, y) \neq A(p_T, b, -y)$, and the interference in Eq. (1) is less than maximal.

There are two theoretical calculations of this interference. Klein and Nystrand [6] calculated the interference using a detailed nuclear form factor, averaging the photon flux over the nucleus. Hencken, Baur, and Trautmann used

a more detailed model of the photon profile and a Gaussian form factor for the nucleus [7]. This work only considered production at midrapidity ($y = 0$), and so cannot be directly compared with the data presented here. At $y = 0$, the two calculations agree quite well.

If the ρ^0 production phase depends on the photon energy, this would introduce a y-dependent phase shift into Eq. (1). This is not expected in the soft-pomeron model [8], and we assume that this phase difference is negligible.

The produced ρ^0's decay almost immediately at two well-separated points, so any interference must develop after the decay, and involve the $\pi^+\pi^-$ final state. Since the pions go in different directions, this requires an entangled $\pi^+\pi^-$ wave function which cannot be factorized into separate π^+ and π^- wave functions; this is an example of the Einstein-Podolsky-Rosen paradox [9,10]. A measurement of the two-source interference is sensitive to any loss of quantum mechanical coherence, be it due to interactions with the environment [11] or as a characteristic of the ρ^0 decay.

Interference is also expected when the ρ^0 photoproduction is accompanied by mutual Coulomb excitation of the two nuclei. This reaction proceeds primarily via three independent single-photon subreactions (one to excite each nucleus, and one to produce the ρ^0) [5]. At a given b, the cross section for the subreactions factorizes; the probability for an n-photon reaction is $P_n(b) = \prod_{i=1}^{n} P_i(b)$ [12], where $P_i(b)$ is the probability for subreaction i. Therefore, these multiphoton reactions have much smaller $\langle b \rangle$, and the effect of interference extends to higher p_T [5]. Because of the different $\langle b \rangle$, multiphoton interactions are important for studying this interference. The Klein-Nystrand model uses measured photonuclear cross sections for the mutual Coulomb excitation [13], while Hencken, Baur, and Trautmann used the giant dipole resonance, plus a correction. For e^+e^- production accompanied by nuclear breakup, using the measured mutual breakup cross sections rather than the Hencken, Baur, and Trautmann approach leads to a 20% larger cross section [14]; a similar difference may apply for ρ^0 photoproduction.

In this Letter we measure two-source interference in 200 GeV per nucleon-pair gold-gold collisions by studying the transverse momentum (p_T) spectrum of photoproduced ρ^0's. These data were taken with the STAR detector. The major detector component used here is a central time projection chamber (TPC) [15] in a 0.5 T solenoidal magnet. The TPC tracked charged particles with pseudorapid-

ity $|\eta| < 1.0$. We used two trigger detector systems, the central trigger barrel (CTB) and two zero degree calorimeters. The CTB consisted of 240 scintillator slats surrounding the TPC, detecting charged particles with pseudorapidity $|\eta| < 1.0$ [16]. The zero degree calorimeters detected neutrons emitted by the dissociating gold nuclei with virtually unchanged longitudinal momentum (100 GeV/c) and low p_T [17].

Data were collected with two different trigger conditions. The first was a topology trigger which selected events with roughly back-to-back pions in the CTB [3]. Nearly vertical pairs were excluded, to reduce contamination from cosmic rays. The second, minimum bias (MB) trigger selected ρ^0 accompanied by mutual dissociation. In these events, both nuclei broke up and released neutrons into the two zero degree calorimeters. The cross section for ρ^0 production accompanied by mutual Coulomb excitation is about 7% [5] of the total ρ photoproduction cross section, so the two data sets are essentially independent.

Events were required to have net charge zero and exactly two reconstructed tracks which formed a vertex less than 50 cm longitudinally from the center of the TPC for the MB sample, and 100 cm for the topology sample. The difference is because events from the CTB based trigger were distributed more broadly along this axis. For the topology data, we exclude events with $|y| < 0.05$ to remove the remaining contamination from cosmic rays, where a single muon track could be reconstructed as two tracks with net charge 0, $p_T = 0$ and $y = 0$. All tracks were assumed to be pions, and were required to have a $\pi\pi$ invariant mass 550 MeV/c^2 < $M_{\pi\pi}$ < 920 MeV/c^2. These criteria produced a clean set of ρ^0 events, at some

cost in efficiency. The 550 MeV/c^2 mass cut removes background from misidentified two-photon production of lepton pairs. The background, estimated from the like-sign pion pairs, was small, 1.4%.

To understand the effect of detector resolution, ρ^0 events were generated following the Klein-Nystrand distributions, and passed through the detector simulation and reconstruction. Figure 1 compares the rapidity and $M_{\pi\pi}$ distributions of the data and simulations. The agreement is good for the minimum bias data, less so for the topology data. This is most likely due to an imperfect topology trigger simulation; the effect of this is treated as a systematic error.

The applied cuts select both directly produced $\pi^+\pi^-$ pairs [18] and ρ^0. Direct $\pi^+\pi^-$ and ρ^0 decays are indistinguishable, so the two processes interfere. The ρ^0 mass peak and direct pion fraction are consistent with earlier gold-gold photoproduction studies [3]. The two subchannels should have the same spin or parity and quantum mechanical behavior, so we do not distinguish between them. If $\pi^+\pi^-$ pairs are produced by a different production mechanism, such as pomeron-odderon interactions [19], then this assumption might not hold.

Figure 2 compares the uncorrected $|\eta| < 0.5$ MB data and simulations based on Refs. [2,5,6] with and without interference, as a function of $t_\perp = p_T^2$. At RHIC energies, the longitudinal component of the 4-momentum transfer is small, so $t_\perp \approx t$. The measured dN/dt spectrum is roughly exponential, but with a significant downturn for $t_\perp < 0.0015$ GeV^2, consistent with the predicted interference. The no-interference histogram is almost exponential, $dN/dt \propto \exp(-kt_\perp)$, where k is related to the nuclear radius [6,20], even though the Klein-Nystrand calculation
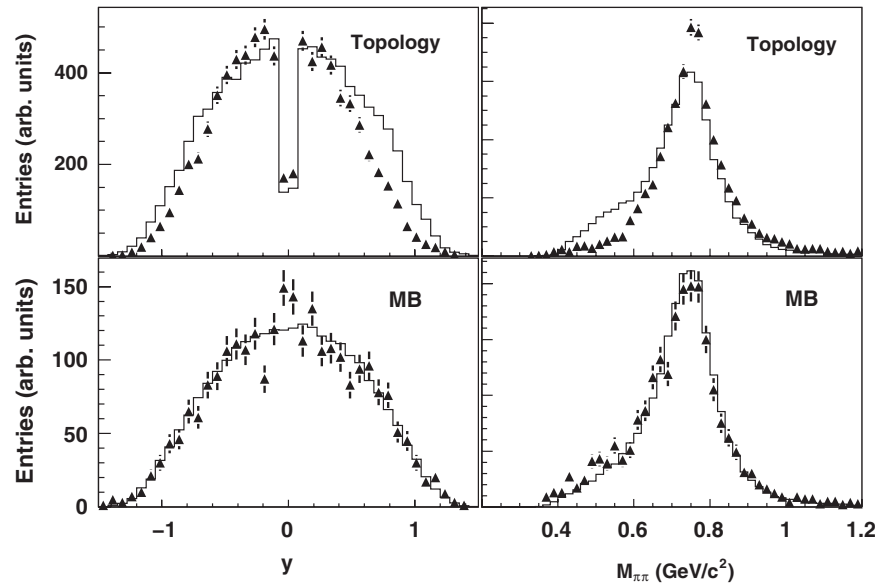

FIG. 1. Rapidity (left) and $M_{\pi\pi}$ (right) of the $\pi^+\pi^-$ distributions for the topology (exclusive ρ^0, top) and MB (Coulomb breakup, bottom) samples. The points with statistical error bars are the data, and the histograms are the simulations. The "notch" in the topology data around $y = 0$ is due to the explicit rapidity cut to remove cosmic-ray backgrounds.
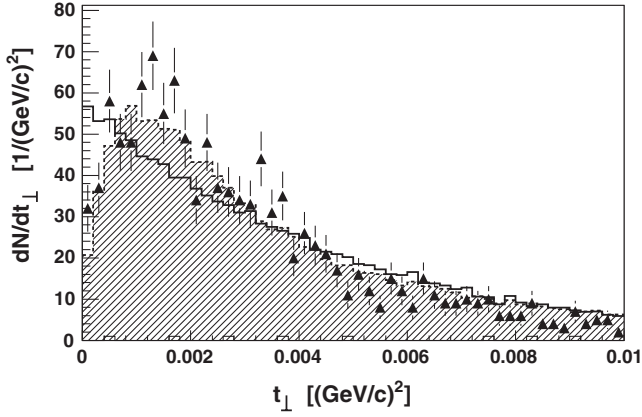
FIG. 2. Raw (uncorrected) ρ^0 $t_\perp$ spectrum in the range $0.0 < |y| < 0.5$ for the MB data. The points are data, with statistical errors. The dashed (filled) histogram is a simulation with an interference term ("Int"), while the solid histogram is a simulation without interference ("NoInt"). The handful of events histogrammed at the bottom of the plot are the wrong-sign ($\pi^+\pi^+ + \pi^-\pi^-$) events, used to estimate the combinatorial background.

uses a Woods-Saxon distribution for the gold density. The Hencken-Baur-Trautmann calculation uses a Gaussian distribution for the nuclear density, but is also fairly well fit by an exponential. The interference in different y ranges is determined using a Monte Carlo simulation which follows the Klein-Nystrand calculations.

Figure 3 shows the efficiency corrected MB and topology data. All four panels show a dip as $t_\perp \rightarrow 0$. As expected, this dip is broader for the MB data because $\langle b \rangle$ is smaller. The suppression at $t_\perp = 0$ is larger for the small-rapidity samples because the amplitudes for the two photon

directions are more similar. The efficiency is almost independent of p_T, so Fig. 2 is not very different from the efficiency corrected $t_\perp$ spectra in Fig. 3. The main effect of the detector response is p_T smearing due to the finite momentum resolution.

The dN/dt spectrum is fit by the 3-parameter form

$$\frac{dN}{dt} = A \exp(-kt)[1 + c(R(t) - 1)], \qquad (3)$$

where

$$R(t_\perp) = \frac{\text{Int}(t_\perp)}{\text{NoInt}(t_\perp)} \qquad (4)$$

is the ratio of the simulated $t_\perp$ spectra with and without interference. For $t_\perp \gg 0.01 \text{ GeV}^2$, $R(t_\perp) \rightarrow 1$, but for $t_\perp \leq 0.01 \text{ GeV}^2$, $R(t_\perp) \neq 1$. A is the overall (arbitrary) normalization, and c gives the degree of spectral modification; $c = 0$ corresponds to no interference, while $c = 1$ is the predicted Klein-Nystrand interference. Table I gives the fit results.

$R(t_\perp)$ was determined using a simulation that includes the detector response, and then fit to two analytic functions: $R(t_\perp) = \Sigma_{i=0}^n a_i/(t_\perp + 0.012 \text{ GeV}^2)^i$ and $R(t_\perp) = \Sigma_{i=0}^n a_i t_\perp^i$. Our results use the first polynomial with $n = 5$; the second polynomial and different values of n were used to estimate the fitting uncertainties.

The weighted average of the four c values is $c = 0.84 \pm 0.05$. The k values for the MB and topology data sets differ by 15%. This may be due to the different b distributions. The photon flux scales as $1/b^2$, so the photon flux on the "near" side of the nucleus is larger than on the "far" side. As b decreases, ρ^0 production is increasingly concentrated on the near side, and the apparent production volume
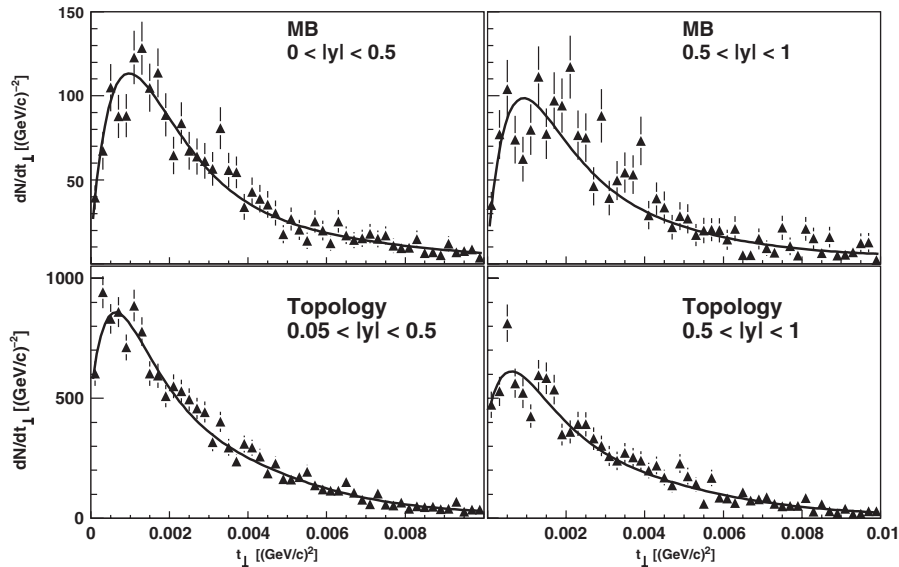

FIG. 3. Efficiency corrected $t_\perp$ spectrum for ρ^0 from (top) minium bias and (bottom) topology data, for midrapidity (left) and larger rapidity (right) samples. The points are the data, while the solid lines are the results of fits to Eq. (3).

TABLE I. The results of fitting Eq. (3) to the four data sets. Here, T is for topology. The $\chi^2/$DOF are discussed in the text (DOF denotes degrees of freedom).

Data set	A	k (GeV^{-2})	c	$\chi^2/$DOF
MB, $\|y\| < 0.5$	$6,471 \pm 301$	299 ± 12	0.92 ± 0.07	$45/47$
MB, $0.5 < \|y\| < 1.0$	$5,605 \pm 330$	303 ± 15	0.92 ± 0.09	$76/47$
T, $0.05 < \|y\| < 0.5$	$11,070 \pm 311$	350 ± 8	0.73 ± 0.10	$53/47$
T, $0.5 < \|y\| < 1.0$	$12,060 \pm 471$	333 ± 11	0.77 ± 0.18	$64/47$

drops, reducing k. A calculation with different assumptions may predict a different electric field variation which leads to a smaller difference in k.

Two of the fits have $\chi^2/$DOF significantly larger than 1. The χ^2 did not decrease with different fit functions for $R(t)$, variations of the nuclear radius in the interference calculations, background level, or modifications to the detector simulation. When the $\chi^2/$DOF > 1, we scale up the fit errors on c by $\sqrt{\chi^2/\text{DOF}}$; this excess error may have theoretical and/or experimental origin. With the scaled errors, the weighted average is $c = 0.86 \pm 0.05$.

Systematic errors come from instrumental effects, background, fitting, and theoretical issues. The major instrumental effects were due to the topology trigger; we apply a 10% systematic error to the topology data to account for this.

This analysis is sensitive to any ρ^0 p_T-dependent efficiency variation. The decay pions have a typical p_T of about 300 MeV/c, where the detection efficiency is high and almost p_T independent [15]. However, the ρ^0 p_T resolution, about 7.5 MeV/c, smears the $t_\perp$ spectrum in the two lowest $t_\perp$ bins. To study detector effects, we fit the raw (uncorrected) $t_\perp$ spectrum with the raw Monte Carlo output; this reduced c by 18% [21], mostly due to the p_T smearing. We assume conservatively that the detector simulation is only 80% effective, and assign a 4% systematic error on c to account for nontrigger detector effects.

Backgrounds were estimated by including like-sign pairs ($\pi^+\pi^+ + \pi^-\pi^-$) in the fits. c changed by less than 0.5%. We assign a 1% systematic error due to backgrounds.

The uncertainty due to fitting was evaluated by comparing results using the two different polynomial forms of $R(t)$ for both $n = 4$ and $n = 5$; c varied by an average of 1%. The effect of an imperfect form factor model was studied by varying the nuclear radius in the simulations. A $\pm 20\%$ change in nuclear radius changed c by 3%. We assign a 4% systematic error due to the fitting procedure.

The theoretical uncertainties are difficult to evaluate. Our simulation follows Refs. [5,6] in detail, but those calculations themselves contain uncertainties. The two theoretical models agree well for exclusive ρ^0 production. For ρ^0 production accompanied by mutual Coulomb excitation, there is some disagreement, but the Klein-Nystrand model has a more detailed excitation calculation, and so may be more accurate. We assign a 5% systematic error due to theoretical issues.

Combining these systematic errors in quadrature results in an 8% (13%) systematic error for the MB (topology) data. Adding the four results in quadrature, including the systematic errors, leads to an interference that is 87% $\pm$ 5%(stat.) $\pm$ 8%(syst.) of the expected level.

Because ρ^0's decay so rapidly, $\gamma\beta c\tau \ll \langle b \rangle$, the ρ^0 decay points are well separated in space-time, and the two amplitudes cannot overlap and interfere until after the decay occurs. The interference must involve the $\pi\pi$ final states [9]. This interference is only possible if the postdecay $\pi\pi$ wave functions retain amplitudes for all possible ρ^0 decays, at least until the wave functions from the two ion sources overlap. The $\pi^+\pi^-$ wave function is not factorizable and is thus an example of the Einstein-Podolsky-Rosen paradox [10]. Unlike previous tests of nonlocality, the interference involves continuous variables, momentum, and position [9].

In conclusion, we have measured the interference between ρ^0 production at two sources (the two nuclei) by observing the $\pi^+\pi^-$ decay products. We observe the interference at 87% $\pm$ 5%(stat.) $\pm$ 8%(syst.) of the expected level. This shows that the final state wave function retains amplitudes for all possible decays, long after the decay occurs. The maximum decoherence (loss of interference) is less than 23% at the 90% confidence level.

[1] C. A. Bertulani, S. R. Klein, and J. Nystrand, Annu. Rev. Nucl. Part. Sci. **55**, 271 (2005); G. Baur *et al.*, Phys. Rep.

364, 359 (2002); F. Krauss, M. Greiner, and G. Soff, Prog. Part. Nucl. Phys. **39**, 503 (1997); K. Hencken *et al.*, Phys. Rep. **458**, 1 (2008).

[2] S. R. Klein and J. Nystrand, Phys. Rev. C **60**, 014903 (1999).

[3] C. Adler *et al.*, Phys. Rev. Lett. **89**, 272302 (2002); B. I. Abelev *et al.*, Phys. Rev. C **77**, 034910 (2008).

[4] L. Frankfurt, M. Strikman, and M. Zhalov, Phys. Rev. C **67**, 034901 (2003); L. Frankfurt, M. Strikman, and M. Zhalov, Phys. Lett. B **537**, 51 (2002).

[5] A. J. Baltz, S. R. Klein, and J. Nystrand, Phys. Rev. Lett. **89**, 012301 (2002).

[6] S. R. Klein and J. Nystrand, Phys. Rev. Lett. **84**, 2330 (2000).

[7] K. Hencken, G. Baur, and D. Trautmann, Phys. Rev. Lett. **96**, 012303 (2006).

[8] T. H. Bauer *et al.*, Rev. Mod. Phys. **50**, 261 (1978).

[9] S. Klein and J. Nystrand, Phys. Lett. A **308**, 323 (2003).

[10] A. Einstein, B. Podolsky, and N. Rosen, Phys. Rev. **47**, 777 (1935).

[11] M. Schlosshauer, Rev. Mod. Phys. **76**, 1267 (2005).

[12] G. Baur *et al.*, Nucl. Phys. **A729**, 787 (2003).

[13] A. J. Baltz, C. Chasman, and S. N. White, Nucl. Instrum. Methods Phys. Res., Sect. A **417**, 1 (1998).

[14] A. J. Baltz, Phys. Rev. Lett. **100**, 062302 (2008).

[15] M. Anderson *et al.*, Nucl. Instrum. Methods Phys. Res., Sect. A **499**, 659 (2003); M. Anderson *et al.*, *ibid.* **499**, 679 (2003).

[16] F. S. Bieser *et al.*, Nucl. Instrum. Methods Phys. Res., Sect. A **499**, 766 (2003).

[17] C. Adler *et al.*, Nucl. Instrum. Methods Phys. Res., Sect. A **470**, 488 (2001).

[18] P. Söding, Phys. Lett. **19**, 702 (1966).

[19] L. Motyka, arXiv:0808.2216.

[20] G. McClellan *et al.*, Phys. Rev. D **4**, 2683 (1971).

[21] S. Klein, for the STAR Collaboration, arXiv:nucl-ex/0402007.